World Academy of Science, Engineering and Technology
International Journal of Agricultural and Biosystems Engineering
Vol:4, No:11, 2010

Wind-Induced Phenomenon in a Closed Water Area with Floating-Leaved Plant

Akinori Ozaki

***Abstract*—**In this study, in order to clarify wind-induced phenomena, especially vertical mixing of density stratification in a closed water area with floating-leaved plants, we conducted hydraulic experiments on wind flow characteristics, wind wave characteristics, entrainment phenomena and turbulent structure by using a wind tunnel test tank and simulated floating-leaved plants. From the experimental results of wind flow and wind wave characteristics, we quantified the impact of the occupancy rate of the plants on their resistance characteristics. From the experimental results of entrainment phenomena, we defined the parameter that could explain the magnitude of mixing between the density stratifications, and quantified the impact of the occupancy rate on vertical mixing between stratifications. From the experimental results of the turbulent structure of the upper layer, we clarified the differences in small-scale turbulence components at each occupancy rate and quantified the impact of the occupancy rate on the turbulence characteristics. For a summary of this study, we theoretically quantified wind-induced entrainment phenomena in a closed water area with luxuriant growth of floating-leaved plants. The results indicated that the impact of luxuriant growth of floating-leaved plants in a closed water body could be seen in the difference in small-scale fluid characteristics, and these characteristics could be expressed using the small-scale turbulent components.

***Keywords*—**Density Stratification, Floating-leaved Plant, Wind-induced Entrainment Phenomenon, Turbulent Structure

I. Introduction

IN a closed water area with little inflow and outflow, the fluids are stratified according to differences in their vertical densities. The density stratification forms due to differences in temperature, turbidity and salt level. The behaviors of the water environmental substances are impacted by turbulent flows caused by wind-induced flow, which is a mechanical disturbance, and convective flow, which is a thermal disturbance. When a wind acts on the water surface of such a closed water area with density stratification, the surface layer becomes turbulent due to the wind action, giving rise to an entrainment phenomenon at the density interfaces. This phenomenon, which results from mixing between the upper and lower water layers, affects the water quality in the closed water area. If there is little turbulence in such a closed water area, little mixing occurs, and the water quality becomes worse.

In a previous study of wind-induced entrainment phenomenon, Mori *et al*. [1] reported that the entrainment phenomenon was governed by the turbulent energy, which accelerated the entrainment, and the stability of stratification, which inhibited the entrainment. The acceleration of the entrainment could be expressed in an entrainment coefficient, and the inhibition of entrainment could be expressed in the Richardson number (a detailed explanation of these terms is given later). The mixing capability between stratifications could be quantified using the relation between the entrainment coefficient and the Richardson number. In addition, Wu, J. [2] and Kit *et al*. [3] clarified the relation between wind-induced potential energy at the water's surface which is caused by the wind current and the Richardson number, and they explained that the entrainment velocity at the boundary of density was governed by the turbulent structure near the boundary of density, which can be attributed to the surface turbulence caused by wind action. Therefore, from the point of view of fluid dynamics, the wind action is to be considered one of the important factors governing the water quality in a closed water area.

When we consider the wind-induced phenomena in closed water areas such as small irrigation ponds and creeks, it is important to consider the impact of floating bodies on fluid movement. Because the fetch is short in closed water areas compared with lakes or dams, floating bodies may significantly decrease the area that can be acted upon by wind. In particular, floating-leaved plants, which have recently begun to be used for water quality purification, may also affect the wind-induced phenomena in a closed water area. To elucidate the mechanism of the entrainment phenomenon, it is important to clarify the relation between the occupancy rate of the floating-leaved plant and wind-induced phenomena in a closed water area.

In this study, in order to clarify the impact of the occupancy rate of floating-leaved plants on wind-induced phenomena in a closed water area, we first conducted an experiment on wind flow on the water surface, wind waves, entrainment phenomenon and turbulent structure by using a wind tunnel test tank. Based on the experimental results, we quantitatively expressed the impact of the occupancy rate of floating-leaved plants on the fluid characteristics that dominate a entrainment phenomenon in a closed water body.

II. Experimental Method

A. Test Tank and Setting Conditions of Plants

The test tank was made of acrylic plate (length 6 meters × width 0.3 meters × depth 0.4 meters). The wind tunnel

Akinori Ozaki is with the Faculty of Agriculture, Kyushu University 812-8581 JAPAN (corresponding author to provide phone: +81-92-642-7159; fax: +81-92-642-7159; e-mail: a-ozaki@agr.kyushu-u.ac.jp).

consisted of a piece of block-board on the test tank (length 6 m × width 0.3 m × depth 0.3 m) (cf. Fig. 1). Instead of using real aquatic plants, we used simulated plants made from polystyrene in the form of plates. The plates had a thickness of 3.0 mm. In this experiment, the occupancy rate as a percentage of the waterway length on the water surface was changed from 0% to 10%, 20%, and 30% (cf. Fig. 2). We set the simulated plants at both ends of the test tank. This reason for this placement was that floating-leaved plants are generally distributed concentric circle-wise from the circumference toward the center in closed water bodies [4].

Regarding the experimental steps, we first examined the wind flow and wind wave characteristics of the test tank using simulated plants and defined the applicable range of wind velocity for this study. In addition, we clarified the impact of simulated plants on wind flow and wave characteristics. Secondly, we conducted an experiment regarding the entrainment phenomenon of two-layered stratified flow and examined the variation of density stratification and turbulent structure. Finally, we theoretically quantified the impact of the occupancy rate of the plants on wind-induced phenomena in a closed water area based on the experimental results.

B. Wind Flow Experiment

The test tank was filled with fresh water. Wind was generated by an air blower. The blowing power was turned up gradually at a specified wind velocity. The measurement values were the vertical wind velocity distribution, the air temperature and water surface velocity. The wind velocity was measured with a hot-wire velocimeter, and the water and air temperature were measured with a thermocouple. The wind velocity distribution, temperature and wave height were measured at two points, 3.0 meters from windward (St. 3.0), 5.0 meters from windward (St. 5.0). In addition, in order to measure the surface flow velocity (U_s), paper with a diameter of 5 mm was floated on the water surface, and the time required for the paper to pass through a fixed zone was measured at St. 3.0. Data from over 30 instances of passage through a fixed zone were collected, although cases in which the paper rode on the wind or on a wave were excluded and we defined the surface flow velocity as passage distance divided by passage time.

C. Wind Wave Experiment

The test tank was the same as in the wind flow experiment. The measurement values were wave profiles. The wave profiles were measured with a resistance wire wave gauge to which two platinum wires were strung. The sampling time for the wave profiles was 120 seconds, and the sampling frequency was 100 Hz. The wave height was measured at 5 points: 2.0 meters from windward (St. A), 3.0 meters from windward (St. B), 4.0 meters from windward (St. C), and 5.0 meters from windward (St. D).

D.Entrainment Phenomenon Experiment

A two-layered, stratified density flow was induced in the test tank. The upper layer contained fresh water, and the lower layer contained salt water. To avoid impulsive breakdown of the density interface, the blowing power was turned up gradually to the specified wind velocity. The measurement parameters were the wind velocity at 0.15 meters above the water surface, and the water temperature and salinity at various increments in the vertical direction. The wind velocity was measured with a hot-wire velocimeter at 2.75 meters from the windward end of the tank, the salinity was measured with a conductance meter, and the water temperature was measured with a thermocouple. The profiles of salinity and water temperature were measured at 3.0 meters from the windward end and the interval between measurements in the vertical direction was 5.0 millimeters.

E. Turbulent Structure Experiment

The equipment and methods were the same as in the entrainment phenomenon experiment. The vertical and horizontal flow components of velocity were measured at 5.0-millimeter intervals from the density interface to the water surface with an X-type hot-wire velocimeter. We set up the velocimeter at two points, 3.0 meters from the windward end of the tank (Point A) and at the edge of the simulated plant (Point B). Since the entrainment phenomenon has an effect on the turbulent structure, we used a sampling time of 30 seconds, and the sampling frequency was 100 Hz.

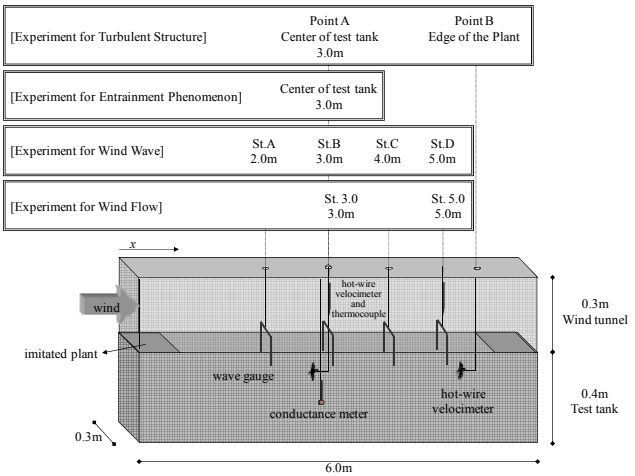

Fig. 1 Schematic diagram of the experimental apparatus

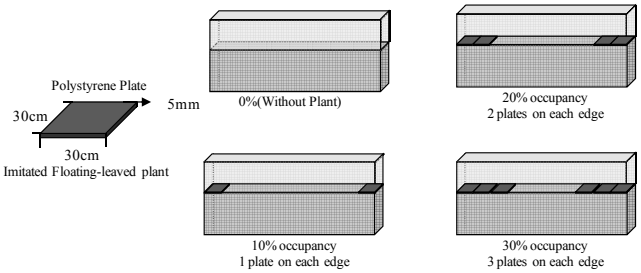

Fig. 2 Method used to simulated floating-leaved plant

III. Experimental Results

A. Results of Wind Flow Experiment

Fig. 3 shows the wind-velocity distributions in the vertical direction as measured at each measurement point for each occupancy rate of the floating-leaved plants. It has previously been reported [5] [6] that the wind distribution near the water surface complied with a logarithmical low, and our results corresponded with this finding. In addition, as the wind velocity increased, the velocity gradient near the water surface became large. These results indicated that the turbulent boundary layer of the wind wave at the water surface was similar to the wall boundary layer. As a consequence, we were able to draw a regression line in these figures, and we calculated the air friction velocity using the following equation:

$$\frac{U(z)}{U_{*a}} = \frac{1}{\kappa}\ln\left(\frac{z}{z_0}\right). \quad (1)$$

where $U(z)$ is the wind velocity at a height z, U_{*a} is the air friction velocity, κ is the Karman constant, z is the height from the water surface, and z_0 is the roughness constant. Fig. 4 shows the relation between the calculated air friction velocity and the wind velocity at 10 m above the water surface, U_{10}, for various conditions of the simulated plant. Here, U_{10} was calculated using the regression expression. As shown in Fig. 4, as the occupancy rate of the plant increased, the air friction decreased slightly at both measurement points. This finding might be explained by the fact that the characteristics of the resistance encountered by air differed between the plant surface and the water surface. Hence, it was necessary to quantitatively elucidate the resistance characteristics of the plants at different occupancy rates. Generally, the vertical transportation of momentum at the water surface is equal to the shear stress acting on the water surface. This transportation is important because of its relation to problems such as the development of wind waves and wind-induced flow. The shear stress, which acts on the water surface, can be expressed in relation to the wind velocity from 10 m above the water surface as follows [7]:

$$C_d = \left(\frac{U_{*a}}{U_{10}}\right)^2. \quad (2)$$

This method is called the Bulk method. Although the Bulk method is usually used when determining the wind-induced flow in the ocean, we used it for calculating the resistance coefficient in the present study because this method makes it easy to derive the formula and because there are many experimental results using this method.

Fig. 5 shows the averaged resistance coefficient under various conditions of the occupancy rate of the plants. Kraus and Turner [8] have reported that when U_{10} ranged from 3 m/s to 16 m/s, the averaged resistance coefficient ran from 1.27×10^{-3} through 1.33×10^{-3}. Our resistance coefficients were slightly greater than the value defined by Kraus and Turner. There were many reasons that there were individual differences between researchers when calculating the resistance coefficient using the logarithmic law. However, our result indicated a difference in the occupancy rate of the plants. The resistance coefficient tended to decrease with increases of the occupancy rate of the plant. Moreover, this tendency was strong at leeward. Therefore, we could conclude that luxuriant growth of floating-leaved plants affects the wind on the water surface. In this study, wind flow was smooth on the simulated plants and met resistance on the water surface.

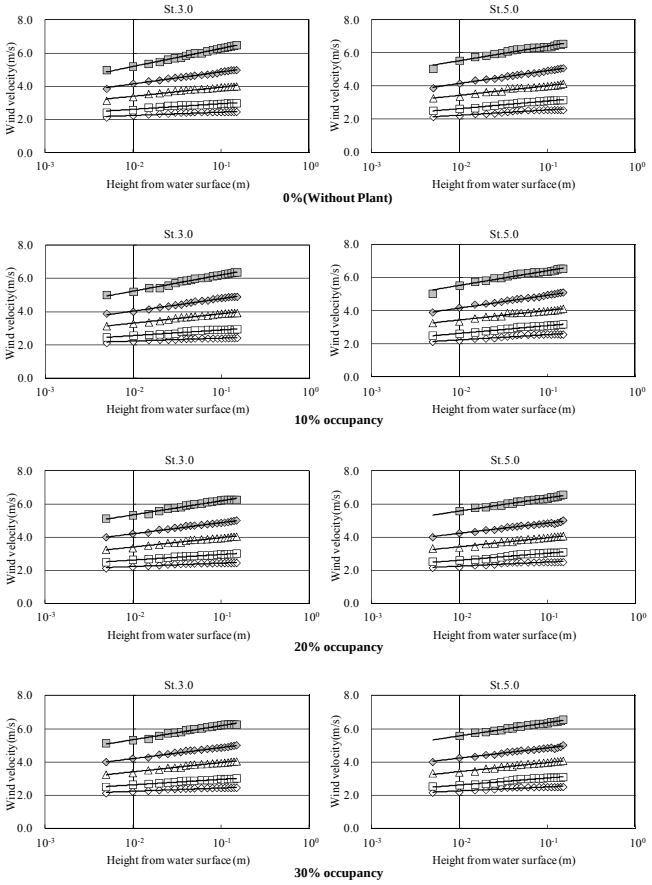

Fig. 3 Wind velocity distribution at each measurement point for each occupancy rate

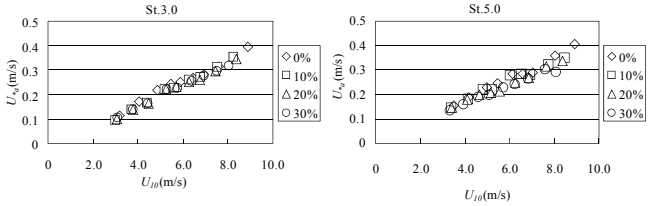

Fig. 4 The relation between calculated air friction velocity U_{*a} and wind velocity at a height of 10m from water surface U_{10} for each occupancy rate

Fig. 6 shows the relationship between surface flow velocity U_s and air friction velocity U_{*a} at St. 3 for each occupancy rate on floating-leaved plants. Regarding the relation between surface

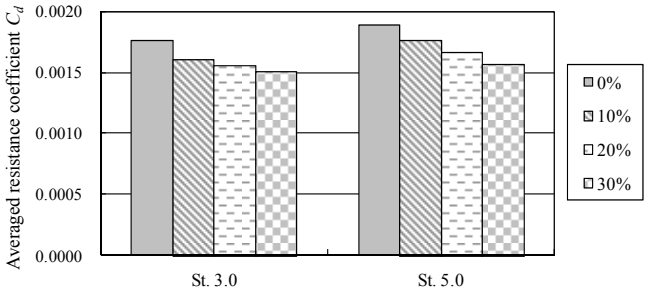

Fig. 5 Averaged resistance coefficient for each occupancy rate

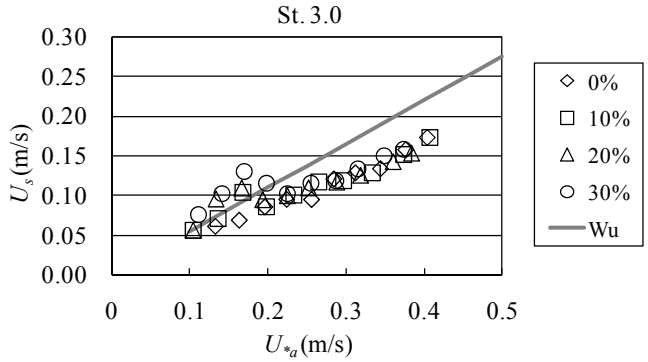

Fig. 6 The relationship between U_{*a} and U_s at St. 3.0 for each occupancy rate

TABLE 1 EXPRESSION FORMULA OF THE RELATION BETWEEN U_s AND U_{*a}

Condition	Relation between U_s and U_{*a}
0%	$U_s = 0.41U_{*a}$
10%	$U_s = 0.38U_{*a}$
20%	$U_s = 0.31U_{*a}$
30%	$U_s = 0.28U_{*a}$
Wu(1975)	$U_s = 0.55U_{*a}$

flow velocity U_s and air friction velocity U_{*a}, Wu [2] has reported that both relations could be expressed as $U_s = 0.55U_{*a}$. Nakayama and Nezu [9] reported that when the wind velocity was relatively great and the wind wave was well developed, both relations approximated the expression formula given by Wu. When compared to the results obtained by Wu, our results with no plant occupancy (0%) were slightly smaller. Therefore, it was considered that in this study the wave did not develop compared with the experimental results of Wu. A comparison of the regression expression calculated by the least-square method of both relations is shown in Table 1. From these results, under the conditions of air friction velocity below 0.23 m/s, both relations were uneven, and these tendencies became stronger as the occupancy rate of the plant increased. Under the conditions of air friction velocity greater than 0.23 m/s, both relations were shown as linear. When the air friction velocity was more than 0.23 m/s, the surface flow velocity increased slightly as the plant occupancy rate increased. This occurred because, when the simulated plants were present on the windward side, the surface occupied by plants was considered to be a smooth region and the water surface was considered to be a rough region. As a result, it was considered that at an air friction velocity below 0.23 m/s, the wind velocity was not sufficient for a wind wave to develop on the water surface, and the floating paper was swept by wind. Moreover, it was found that an air friction velocity of 0.23 m/s or more was required to cause a wind wave to develop.

B. Results of Wind Wave Experiment

Generally, the characteristics of the power spectrum distribution are well known to express the statistical characteristics of a wave. In this study, we used the power spectrum obtained in the experiment for verification of the wind wave. We divided all of the obtained data, i.e. the data calculated using FFT, into 2048 data blocks, and performed the spectrum calculation by obtaining an ensemble average of the results of FFT. Regarding the form of the power spectrum, it is well known that the results of spectrum analysis of well-developed waves comply with the following equation on the high frequency side:

$$\phi(f) = \beta g^2 f^{-5}. \quad (3)$$

where $\phi(f)$ is the power spectrum, g is the acceleration of gravity, f is the frequency and β is the constant $(=9.51\times10^{-3})$. Fig. 7 shows the calculated results of the power spectrum for the occupancy rates of 0% and 20%. Our calculated result did not comply with this equation on the high frequency side at St. A. This lack of compliance could be explained by the fact that the wave was in its early stage of development and was too small to measure with our wave gauge. The same reason for the lack of compliance with this equation could be given for the experimental cases in which the representative wind velocity was below 4.0 m/s. Therefore from the results of the analysis of the power spectrum of the wind wave suggest that the waveform data obtained in these experiments were consistent with the presence of waves except the data measured at St. A and the experimental cases with a representative wind velocity below 4.0 m/s. On the other hand, at St. B, St. C, and St. D and in the experimental cases with a representative wind velocity over 4.0 m/s, the calculated result complied with this equation. In the experimental case with a representative wind velocity of 4.7 m/s, β showed the best agreement with the equation, and when the value of the representative wind velocity increased to more than 4.7 m/s, β tended to become large. In addition, as the representative wind velocity became higher and the fetch became longer, the peak of the power spectrum moved to the low frequency side at each occupancy rate. Moreover, as the occupancy rate of the plant increased, the power spectrum values decreased. These results meant that increases of wind velocity and of the length of the fetch had the same effect on the development of the spectrum, and the peak of the power spectrum moved to the low frequency side with the development of the spectrum. As

compared with the results of the experimental cases with 0% and 20 % occupancy rates, the power spectrum at an occupancy rate of 20% was low value, and the development rate of the wind wave was low. Therefore, it was considered that the existence of the plant reduced the wind energy and inhibited the development of the wind wave.

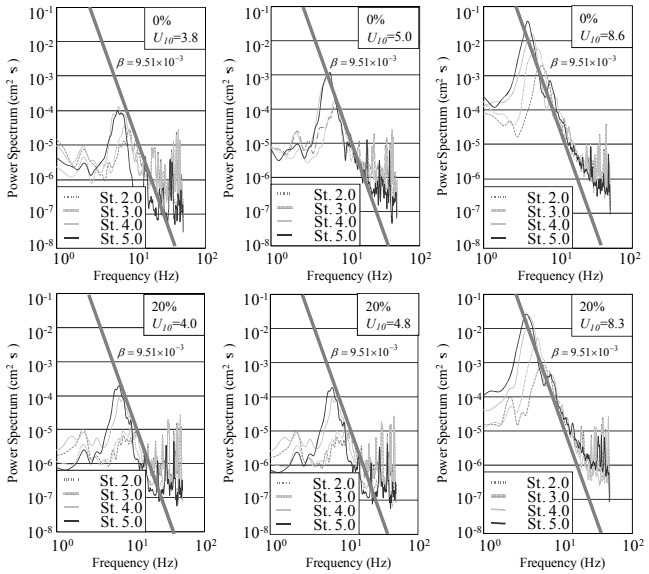

Fig. 7 Power spectrum distributions for experimental case 0% and 20% occupancy rate

C. Results of the Entrainment Phenomenon Experiment

Entrainment velocity is generally given by the coefficient of entrainment E and the over-all Richardson number R_{ia}, which are defined as

$$E = \frac{U_e}{V}. \tag{4}$$

$$R_{ia} = \frac{\Delta\rho g h}{\rho V^2}. \tag{5}$$

where U_e is the entrainment velocity, V is the reference velocity of flow, h is the water depth of the upper layer, ρ is the reference density, $\Delta\rho$ is the density difference between the upper and lower layers, and g is the gravitational acceleration. When the water flow is two-dimensional and the section of flowing water under consideration is rectangular, the continuity equation of the flow rate and the density conservation law for the upper layer are respectively given as

$$\frac{\partial h_1}{\partial t} + \frac{\partial (u_1 h_1)}{\partial x} = U_e. \tag{6}$$

$$\frac{\partial (\rho_1 h_1)}{\partial t} + \frac{\partial (\rho_1 u_1 h_1)}{\partial x} = \rho_2 U_e. \tag{7}$$

where u_1 is the cross-average velocity of the upper layer, h_1 is the upper water depth, ρ_1 is the density of the upper layer, ρ_2 is the density of the lower layer, x is the mainstream direction, and t is time. In wind-induced flow, the second term on the left-hand side of Eq. (6) is small. Hence the entrainment velocity is able to represent the rate of variation of the upper water depth with time, i.e., the descending velocity of the density interface, as shown below:

$$\frac{dh_1}{dt} = U_e. \tag{8}$$

Eq. (7) and $\Delta\rho = \rho_2 - \rho_1$ yield

$$\frac{\partial \rho_1}{\partial t} + u_1 \frac{\partial \rho_1}{\partial x} = \frac{\Delta\rho}{h_1} U_e. \tag{9}$$

If the lower water entrained to the upper layer is rapidly and uniformly mixed and diffused in the vertical and horizontal directions, the second term on the left-hand side of Eq. (9) can be omitted.

$$\frac{d\rho_1}{dt} = U_e \frac{\Delta\rho}{h_1}. \tag{10}$$

By performing integration under the condition that ρ_2 is constant, we obtain the following from Eq. (8) and Eq. (10)

$$h_1 \Delta\rho = h_i \Delta\rho_i = const. \tag{11}$$

where h_i is the initial upper water depth and $\Delta\rho_i$ is the initial difference in density between the upper and lower layers. Hence we can substitute as follows:

$h \to h_i$, $\Delta\rho \to \Delta\rho_0$, $\rho \to \rho_a$, $V \to U_{*a}$.

where $\Delta\rho_0$ is the initial density difference of the layers, U_{*a} is the air share velocity and ρ_a is the air density. Thus Eq. (4) and Eq. (5) can be described below as a time-invariant equation

$$R_{ia} = \frac{\Delta\rho_0 g h_i}{\rho_a U_{*a}^2}, \tag{12}$$

and, by Eq. (8), the coefficient of entrainment E can be described as

$$E = \frac{dh_i / dt}{U_{*a}} = \frac{U_e}{U_{*a}}. \tag{13}$$

In this study, we considered the results of the entrainment phenomenon experiment by using R_{ia} and E, which were obtained by Eq. (12) and Eq. (13), respectively.

Fig. 8 shows the variation rate of the upper water layer with time; the depth represents the height of the density interface. Shortly after the wind blowing the rate was variable because the formation of circulation flow and the development of internal waves did not occur; however, the rate was linearly proportional to time. Since a previous experiment without plants [1] had shown the same tendency, we could conclude that the lowering of the velocity of the density interface was constant except shortly after the wind blowing. Hence the entrainment velocity U_e in the present experiment could also be described as $U_e \equiv dh/dt = const$.

Fig. 9 shows the relationship between the entrainment coefficient E and the over-all Richardson number R_{ia} in the present experiment. The entrainment coefficient E can express the magnitude of the entrainment phenomenon, and the over-all Richardson number R_{ia} can express the intensity of density stratification. From Fig. 9 the entrainment coefficient E in the

TABLE II EXPERIMENTAL CONDITIONS FOR ENTRAINMENT PHENOMENON

Run No.	Occupancy rate	$U_{0.15}$ (m/s)	$\Delta\rho\times10^3$ (kg/m^3)	ρ_a (kg/m^3)	h_i (m)	U_{*a} (m/s)	R_{ia}
1	0%	6.1	0.0022	1.169	0.110	0.242	34.4
2		8.0	0.0032	1.171	0.120	0.353	25.4
3		5.9	0.0052	1.168	0.100	0.231	92.1
4		7.9	0.0045	1.171	0.120	0.347	37.1
5		6.2	0.0027	1.208	0.104	0.247	59.2
6		6.0	0.0055	1.168	0.100	0.236	82.1
7	10%	7.2	0.0027	1.181	0.110	0.305	26.6
8		6.0	0.0017	1.168	0.100	0.236	25.8
9		8.3	0.0076	1.173	0.116	0.432	39.6
10		7.7	0.0021	1.198	0.158	0.395	17.6
11		8.4	0.0107	1.195	0.084	0.401	45.7
12	20%	6.0	0.0032	1.176	0.104	0.261	41.2
13		7.5	0.0080	1.183	0.107	0.372	51.5
14		8.1	0.0048	1.190	0.109	0.360	33.2
15		7.7	0.0027	1.194	0.141	0.389	20.7
16		7.8	0.0021	1.192	0.113	0.401	12.1
17	30%	7.5	0.0060	1.194	0.094	0.382	31.5
18		7.7	0.0054	1.208	0.100	0.395	27.9
19		8.1	0.0037	1.202	0.100	0.419	17.0
20		7.9	0.0028	1.197	0.100	0.408	15.3

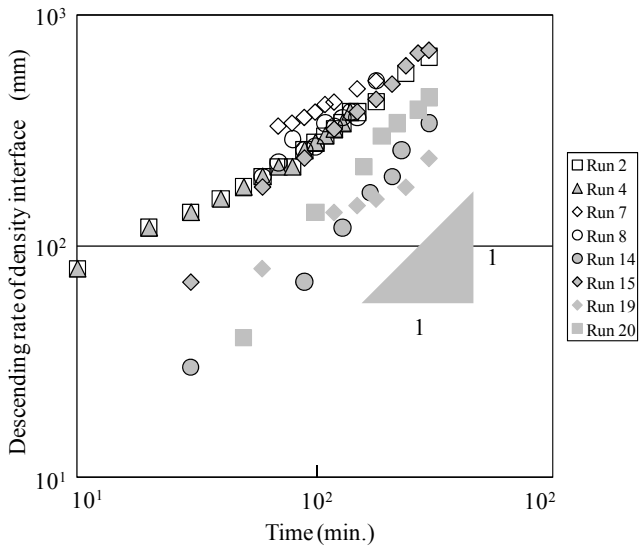

Fig. 8 Rate of decent of the density interface with time for various overall Richardson numbers R_{ia}

experiment with simulated plants was much lower than in the experiment without plants. And the larger the occupancy rate of the plants became, the lower the entrainment velocity became. Regarding the relationship between E and R_{ia}, the previous results of $E \propto R_{ia}^{-3/2}$ for an experiment without aquatic plants [1] complied with the whole setting conditions of the simulated plant for the values of R_{ia} ranging from 0 to 100. In addition, it was reported in this previous experiment that the constant of proportion, which was obtained from the relation between E and R_{ia}, could express a magnitude of vertical mixing between the upper and lower layers at the density interface. As a representative velocity for defining E and R_{ia}, Takahashi and Suga [10] used mean flow velocity to represent the main stream direction U_m, Kit *et al.* [3] used the backward flow velocity near the density interface U_{ri}, and Ura [11] used the uniformity flow velocity for backward flow, and and these previous researchers all estimated the magnitude of vertical mixing by using the constant of proportion obtained from the relation between E and R_{ia}. In the present study, we used the air friction velocity U_{*a} as the representative flow velocity, and we quantitatively estimated the magnitude of vertical mixing for each occupancy rate of the plant by using the following equation.

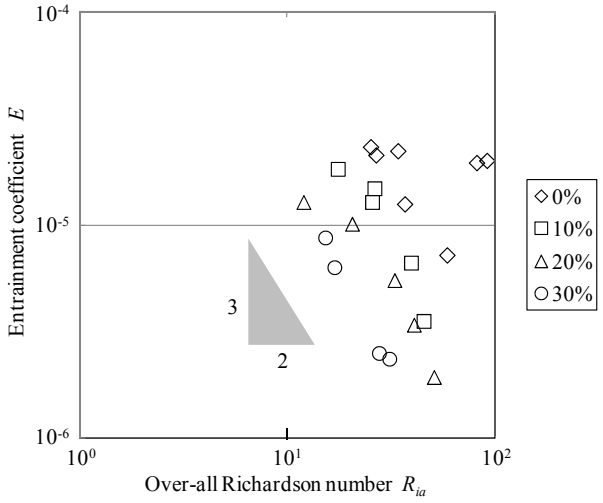

Fig. 9 Entrainment rate E plotted logarithmically against over-all Richardson numbers R_{ia}

TABLE III EXPRESSION FORMULA OF THE RELATION BETWEEN E AND R_{ia}

Condition	Relation between E and $R_{ia}^{-3/2}$
0%	$U_e/U_{*a}=0.76\times10^{-2}\left(\Delta\rho gh/U_{*a}^2\right)^{-3/2}$
10%	$U_e/U_{*a}=0.16\times10^{-2}\left(\Delta\rho gh/U_{*a}^2\right)^{-3/2}$
20%	$U_e/U_{*a}=0.08\times10^{-2}\left(\Delta\rho gh/U_{*a}^2\right)^{-3/2}$
30%	$U_e/U_{*a}=0.04\times10^{-2}\left(\Delta\rho gh/U_{*a}^2\right)^{-3/2}$
Takahashi et al.	$U_e/U_m=2.0\times10^{-3}\left(\Delta\rho gh/U_m^2\right)^{-3/2}$
Kit et al.	$U_e/U_{ri}=2.0\times10^{-1}\left(\Delta\rho gh/U_{ri}^2\right)^{-3/2}$
Ura	$U_e/U_r=5.0\times10^{-2}\left(\Delta\rho gh/U_r^2\right)^{-3/2}$

$$\frac{U_e}{U_{*a}}=K\left(\frac{\Delta\rho gh}{U_{*a}}\right)^{-3/2} . \quad (14)$$

Table 3 shows the constant of proportion K which was obtained by Eq. (14). From Table 3, the magnitude of vertical mixing between the upper and lower layers was exponentially decreased as the occupancy rate of the plant increased.

D.Results of Turbulent Structure Experiment

Fig. 10 shows the profiles of the time-average velocity in the horizontal direction $\overline{U}$ for the various values of the occupancy rate. In Fig. 10, the horizontal axis represents the dimensionless time-average flow rate in the horizontal direction, and the

vertical axis represents the dimensionless upper layer water depth. The wind direction was from the left side to the right side in these figures. The expression $z/h_i = 1$ represents the water surface and $z/h_i = 0$ represents the density interface. In these figures U_s represents the flow velocity of the water surface, z is the measurement height and h_i is the upper layer water depth. From Fig. 10, it can be seen that as the occupancy rate of the plant became large, the horizontal flow velocity $\overline{U}$ at each measured point tended to decrease. At point A, the turning point from the wind-driven current to the return current moved toward the water surface with an increase in the occupancy rate. At point B, the occupancy rate of the plant became large, and the wind-driven current became a gentle flow. The return current was uniform except in the experiment without the plants, because in that experiment the horizontal flow velocity was affected by the wall.

Fig. 11 shows the profiles of the time-average velocity in the vertical direction $\overline{V}$ for the various values of the occupancy rate. In Fig. 11, the horizontal axis represents the dimensionless time-average flow rate in the vertical direction, and the vertical axis represents the dimensionless upper layer water depth. The vertical flow velocity defines the upward flow that goes from the density interface to the water surface as positive. From Fig. 11, since the value in the upper 20-30% of the depth of the water

TABLE IV EXPERIMENTAL CONDITIONS FOR TURBULENT STRUCTURE

Run No.	Occupancy rate	U_{10} (m/s)	$\Delta\rho \times 10^3$ (kg/m^3)	ρ_a (kg/m^3)	h_i (m)	U_{*a} (m/s)	U_* (m/s)	R_{ia}
1	0%	8.5	0.0118	1.237	0.126	0.445	0.017	59.3
2	10%	8.3	0.0115	1.237	0.096	0.432	0.015	46.4
3	20%	8.3	0.0106	1.236	0.101	0.432	0.015	45.5
4	30%	8.5	0.0111	1.237	0.108	0.445	0.015	48.1

was affected by wind, the value of the time-average velocity was high and spread. The flow direction that sank from the water surface to the density interface was high values. And the values became almost 0 uniformly under about 50 percent of the upper water depth. In addition, it was likely that the velocity in the vertical direction differed because the representative scale changed with the wind velocity. The time-average vertical velocity did not show a systematic difference under each occupancy rate of the plants because the sampling time of the hot-wire velocimeter was not particularly long. No large differences were observed between the measured values at any point.

From the above comparison of the mean flow velocity for the horizontal and vertical directions, it was found that the impact of the occupancy rate of the plants on flow velocity was not great. This meant that the dominant factor of the entrainment phenomenon was considered to be a small-scale phenomenon.

In order to clarify the impact of this small-scale phenomenon, we examined the turbulent intensity which was obtained by analyzing the fluctuation of flow velocity. Fig. 12 shows the

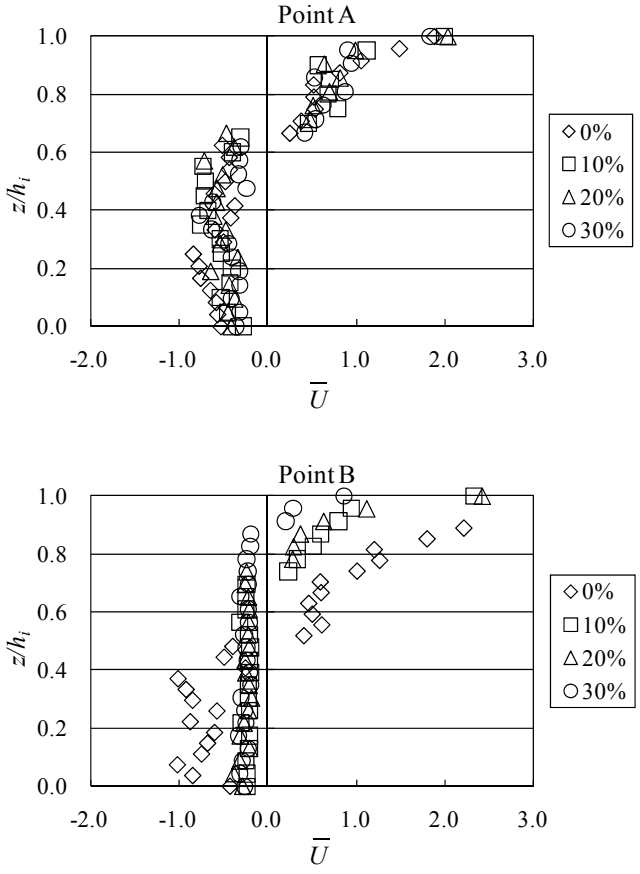

Fig. 10 Time-averaged velocity profiles in the horizontal direction

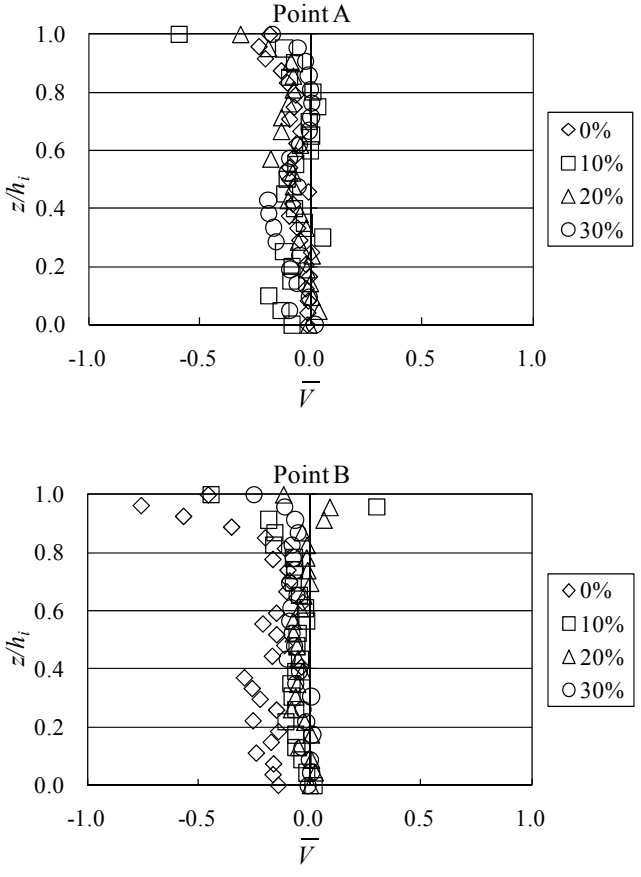

Fig. 11 Time-averaged velocity profiles in the vertical direction

relationship between the horizontal and vertical turbulent intensities averaged with the upper water depth and the various occupancy rates. In these figures,

$$\widetilde{U} = \frac{1}{h_1 U_*}\int_0^{h_1}\sqrt{\overline{U'}^2}\,dz \ , \tag{15}$$

$$\widetilde{V} = \frac{1}{h_1 U_*}\int_0^{h_1}\sqrt{\overline{V'}^2}\,dz \ . \tag{16}$$

where U' is the turbulent component of the horizontal direction, V' is the turbulent component of the vertical direction, and U_* represents the friction velocity at the water surface. In Fig. 12, the horizontal and vertical turbulent intensities averaged with water depth became smaller as the occupancy rate became larger. These figures corresponded with the change of K, which was obtained from the experimental value for the entrainment phenomenon. It was concluded that the vertical mixture capability between the vertical layers declined as the water surface occupied by the plant became large. Namely, the magnitude of the turbulent intensity became small because the upper turbulent structure changed.

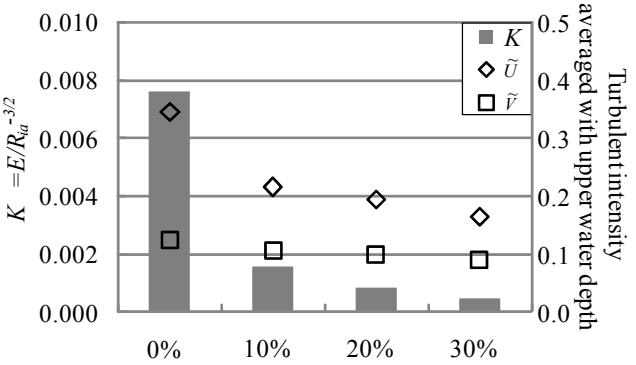

Fig. 12 Turbulent intensity averaged with upper water depth and constant of proportion K

IV. Theoretical Quantification for Wind-Induced Entrainment Phenomenon

In order to express the entrainment phenomenon at the density interface quantitatively, we considered the contribution of the work done by wind stress to the increases in potential energy at the density interface. Fig. 13 shows a definition sketch of the change in the potential energy due to the wind-induced flow where the mixing layer is seen to be deepened by dh in a period of dt. If we designate that, at time t, ρ is the density of the mixed fluid and $\Delta\rho$ is the density difference at the density interface, the rate of change dE_p/dt of the potential energy per unit surface area can be written as

$$\frac{dE_p}{dt} = \frac{1}{dt}\left[\left(\frac{dh\Delta\rho}{h}\right)g(h+dh)\left(\frac{h+dh}{2}\right)\right]. \tag{17}$$

Neglecting the higher order terms, we obtain

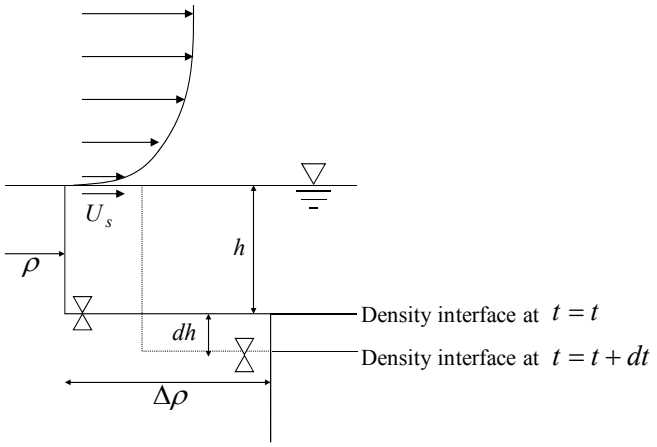

Fig. 13 Definition sketch of the change in the potential energy due to the wind-induced flow

$$\frac{dE_p}{dt} = \frac{1}{dt}\times\frac{1}{2}\Delta\rho g h dh \ . \tag{18}$$

The rate dE_k/dt of work done by the wind stress per unit surface area is generally expressed [8] as

$$\frac{dE_k}{dt} = \tau_s U_s = \rho_a {U_{*a}}^2 U_s \ . \tag{19}$$

where, τ_s is the wind stress and U_s is the s surface flow velocity. By comparing the rate of increase of the potential energy of the mixing layer due to the rate of work done by the wind stress, we can determine the fraction of the work done by the wind used for mixing at the density interface. From (18) and (19), we obtain

$$\frac{dE_p}{dE_k} = \frac{1}{2}\times\frac{\Delta\rho g h dh}{\rho_a {U_{*a}}^2 U_s dt} \tag{20}$$

In this formula,

$$\frac{\Delta\rho g h}{\rho_a {U_{*a}}^2} = R_{ia} \ , \tag{21}$$

and

$$\frac{dh}{dt}\times\frac{1}{U_{*a}} = E \ . \tag{22}$$

We rewrite Eq. (20) by using Eq. (21) and Eq. (22), and we obtain

$$\frac{dE_p}{dE_k} = \frac{1}{2}ER_{ia}\frac{U_{*a}}{U_s} \ . \tag{23}$$

Mori *et al.* [1] have reported that when $R_{ia} < 100$ the relation between dE_p/dE_k and $R_{ia}^{-1/2}$ can be drawn as $dE_p/dE_k \propto R_{ia}^{-1/2}$. So from this relation

$$\frac{dE_p}{dE_k} = \frac{1}{2}ER_{ia}\frac{U_{*a}}{U_s} \propto R_{ia}^{-1/2} \ . \tag{24}$$

From Eq.(24)

$$E = \alpha\frac{U_s}{U_{*a}}\times R_{ia}^{-3/2} \ . \tag{25}$$

where α is a constant of proportion. That is, we can express K, which represents the entrainment scale at the density interface, as the ratio of the flow velocity at the water surface and air friction velocity. In addition, Ura [11] has reported that the elements that determined K included the turbulent intensity, integral scale, and eddy scale, which act on the density interface, and the wavelength and wave height of variation of the density interface. Ura defined these relations as a turbulent coefficient by using the following equation:

$$T = \left(\frac{U'}{U_M}\right)^4 \cdot \left(\frac{l}{h}\right)^{-3/2}. \quad (26)$$

where U' is the turbulent intensity, U_M is the mean flow velocity of the upper layer, l is the integral scale of the turbulent intensity and h is the depth of the upper layer. The integral scale of the turbulent intensity l was defined using the following equation,

$$l = \frac{1}{\overline{U'}} \int_0^{20} R(\tau) d\tau. \quad (27)$$

where $R(\tau)$ is an autocorrelation function defined in the following equation,

$$R(\tau) = \overline{U'(t+\tau)\, U'(t)}. \quad (28)$$

Fig. 14 shows the relationship between K, which was defined based on the experimental results of the entrainment phenomenon, and T which was defined by Eq. 26. This figure shows that as the occupancy rate of the plant increased, the values of K and T decreased. In an experimental case without plants, Ura found the relation between K and T to be $K/T = 0.7$. Our experimental results in the case without plants showed the value of K/T to be quite similar to this value. As the occupancy rate of the plant increased, the turbulent coefficient T decreased along with K. Therefore, we could explain the decrement of the entrainment near the boundary of the density and the attenuation of the turbulent components due to the occupancy of the floating-leaved plants by using the turbulent coefficient T and K/T.

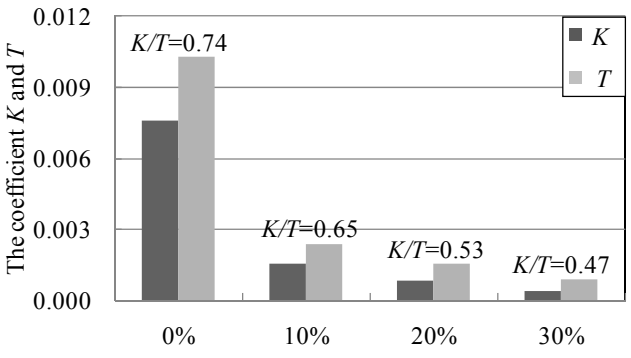

Fig. 14 The relationship between, K which was defined based on the experimental results of entrainment phenomenon and turbulent coefficient T

V. CONCLUSION

From this study, we could conclude that luxuriant growth of floating-leaved plants in a closed water body affected the wind flow characteristics and wind wave characteristics by decreasing the length of the fetch. Furthermore, the energy levels of the diffusing layer and the entrainment layer were attenuated by the attenuation of the wind-driven current, i.e., the surface shearing layer, as the response of the floating-leaved plants affected the water surface. Therefore, it can be concluded that when floating-leaved plants grow on the water surface in a closed water body, the entrainment velocity decreases as the occupancy rate increases.

It is thought that the plants affect the turbulence induced by wind and cause the water quality to decrease.

Consequently, when floating-leaved plants are used as a purification technique to improve water quality, we recommend maintaining the water surface area so that it can be acted upon by the wind.

REFERENCES

[1] Mori, K., Tohara, Y. and Kato O "Experimental Research of Entrainment Rate of Density Interface due to a Wind Induced Current" *Transaction of the Japanese society of irrigation, drainage and reclamation engineering.* 1989, Vol. 144, pp.85-93

[2] Wu, J. "Wind-Induced Turbulent Entrainment Across a Stable Density Interface", *Journal of Fluid Mechanics*, 1973, 61, pp. 275-287.

[3] Kit,E., Berent,E. and Vajda,M. "Vertical Mixing Induced by Wind and a Rotating Screen in a Stratified Fluid in a Channel", *Journal of Hydraulic Research*. 1980, 18, pp.35-58

[4] Ikushima, K. "Substance Production of Plant Community near Water", Kyoritsu Publishing, Tokyo, 1974

[5] Shemdin,O.H. "Wind-Generated Current and Phase Speed of Wind Waves". *Journal of Physical Ocean,* 1972, 2, pp.411-419

[6] Wu, J. "Wind-Induced Drift Currents". *Journal of Fluid Mechanics*, 1975, 68,pp.49-70

[7] Tsuruya, H. "Experimental Study of Wind Driven Currents in a Wind-Wave Tank -Effect of Return Flow on Wind Driven Currents-", *Report of the Port and Harbor Research Institute*, 1983, Vol.22, No.2, pp.128-174

[8] Kraus, E.B. and Turner, J.S. "A One-Dimensional Model of the Seasonal Thermocline The general theory and its consequences", *Tellus*, 1967, 19, pp. 98-106

[9] Nakayama, T. and Nezu, I. "Turbulence Structure of Wind Water Waves", *Journal of Japan Society of Civil Engineering*, 2000, No.642, II -50, pp. 45-56

[10] Takahashi, A. and Suga, A. "Entrainment Coefficient in the Salt-Water Fresh-Water Stratification", *Proceedings of Annual Conference of the Japan Society of Civil Engineers,* 1976, No.2, pp383-384

[11] Ura, M. "Variation of Density Interface and Entrainment Velocity Induced by Wind Shear", *Proceedings of Coastal Engineering. JSCE*. 1983, Vol.30, pp.561-565